Climate Dynamics (2020) 54:525–541
https://doi.org/10.1007/s00382-019-05013-7

The non-linear relationship between the western North Pacific anticyclonic circulation and Korean summer precipitation on subseasonal timescales

Sae-Rim Yeo[1] · MinHo Kwon[2] · June-Yi Lee[3,4]

Received: 20 May 2019 / Accepted: 10 October 2019 / Published online: 29 October 2019

Abstract
It has been widely known that the pulse of the western North Pacific anticyclonic circulation (WNPAC) plays a key role on East Asian summer climate variability in subseasonal to interannual time scales. Yet, the relation between the WNPAC and summer precipitation over Korea is not robust on seasonal and subseasonal timescales for the recent few decades. Here, we show that the low correlation between WNPAC and Korean precipitation is attributable to their distinctive non-linear relationship and investigate detailed features in their four different phase relationships on subseasonal time scales. First, the positive Korean precipitation anomaly occurs as the part of zonally elongated precipitation band along with the positive WNPAC anomaly closely connected with the decaying phase of El Niño and Indian Ocean warming. The second case is enhanced Korean precipitation accompanying with negative WNPAC anomaly. In this case, the negative WNPAC anomaly constitutes a part of atmospheric wave train across the North Pacific and this feature is associated with the decaying phase of La Niña. The typhoon-related precipitation event also contributes to this case. Third, the negative Korean precipitation anomaly arises when the low-level easterly anomaly along with the northern flank of negative WNPAC anomaly leads to suppressed convective activity in Korea. Lastly, the negative Korean precipitation anomaly happens with the positive WNPAC anomaly when anomalous high covers entire East Asia and the WNP mainly during the decaying phase of central Pacific El Niño. The understanding of the non-linear relationship between WNPAC and Korean precipitation in this study provides better insight into the potential impacts of El Niño-Southern Oscillation and circulation/convection anomaly over the WNP on summer Korean precipitation.

1 Introduction

Korean summer precipitation accounts for more than half of the annual precipitation amount and exerts profound socioeconomic impacts over Korea (e.g., Lee et al. 2017). Therefore, better understanding on underlying mechanisms of Korean summer precipitation variability and improving their predictability meet forefront scientific and societal needs. Summer precipitation in Korea especially Changma, which is the successive rainy period, has been considered as one of major sub-monsoon components in East Asian summer monsoon (EASM) system. Previous studies on Korean summer precipitation variability have been generally conducted in the framework of EASM (e.g., Kang et al. 1999; Park et al. 2015).

Numerous studies have attributed the EASM variability to the sea surface temperature (SST) variation over the tropical oceans (e.g., Huang and Wu 1989; Zhang et al. 1996). In particular, the effects of El Niño-Southern Oscillation (ENSO) (Nigam 1994; Wang et al. 2000; Wu et al. 2003) and Indian Ocean (Guan and Yamagata 2003; Li et al. 2008; Xie et al. 2009) have been extensively discussed. It has been widely recognized since the pioneering work of Wang et al. (2000) that the key system that connects ENSO and Indian Ocean variability to EASM is the variability of the western North Pacific (WNP) anticyclonic circulation (WNPAC).

✉ Sae-Rim Yeo
sryeo@apcc21.org

[1] APEC Climate Center, Busan, Republic of Korea

[2] Korea Institute of Ocean Science and Technology, Busan, Republic of Korea

[3] Research Center for Climate Sciences and Department of Climate System, Pusan National University, Busan, Republic of Korea

[4] Center for Climate Physics Institute for Basic Science (IBS), Busan, Republic of Korea

The positive WNPAC anomaly emerges from the mature phase of El Niño during winter via local ocean–atmosphere interaction (Wang et al. 2000; Lau and Nath 2003), and it peaks during following spring through wind-evaporation-SST feedback (Wang et al. 2000). The persistence of positive WNPAC anomaly during summer, on the other hand, is largely affected by Kelvin wave induced Ekman divergence from Indian Ocean warming (Yang et al. 2007; Xie et al. 2009; Wu et al. 2010). In addition, the convective activity over the WNP significantly regulates the WNPAC variability and it often features meridional wave-like atmospheric structure from tropics to East Asia, which is known as Pacific–Japan (PJ) pattern (Nitta 1987; Huang and Sun 1992; Kosaka and Nakamura 2006).

Along with the western flank of the WNPAC, the large amount of water vapor can be transported from tropics to East Asia through the southwesterly flow. In general, the enhanced WNPAC leads to strengthening of the EASM. As such, the WNPAC acts as an atmospheric bridge that links tropical variability to EASM (Lu 2001; Lu and Dong 2001; Wang and Zhang 2002; Lee et al. 2006, 2013; Park et al. 2010; Yeo et al. 2012; Wang et al. 2013). Based on the general consensus on the crucial role of WNPAC in affecting EASM, a number of attempts have been made to predict EASM using WNPAC variability (e.g., Chowdary et al. 2011; Wang et al. 2013, 2015). For example, based on high correlation coefficient between WNPAC index and EASM intensity, Wang et al. (2013) established the prediction model of WNPAC, which can be directly applied to EASM prediction.

Despite the considerable efforts have been made to understand the linkage between WNPAC and EASM, the relationship between regional Korean summer precipitation and WNPAC has not been sufficiently elucidated in the previous studies. In particular, less attention has been paid to the relationship on subseasonal time scales in spite of their considerable subseasonal variability (e.g., Kim et al. 2011; Yeo et al. 2012; Lee and Seo 2013). Although Korean summer precipitation is a vital part of EASM, it also exhibits distinctive regional characteristics from EASM variability, which is largely due to its geographical location (Lee and Seo 2013; Park et al. 2015). Indeed, simple correlation analysis reveals that there is no significant linear relationship between Korean summer precipitation and WNPAC on subseasonal as well as seasonal time scales (see Sect. 3 for more detailed explanation). This result suggests that more comprehensive understanding on the relationship between Korean summer precipitation and climate variability over WNP should be addressed.

The main purpose of the present study is, therefore, to investigate detailed physical relationship between Korean summer precipitation and WNPAC. Especially, it is found that the low correlation between WNPAC and Korean summer precipitation is attributable to a distinctive non-linear relationship between them. Therefore, the characteristics of atmospheric and oceanic variations for four different phase relationship between WNPAC and Korean precipitation are investigated. Considering the large subseasonal variations of both Korean summer precipitation and WNPAC, this study investigates the relationship between WNPAC and Korean summer precipitation on subseasonal time scale and thus the analyses are mainly conducted on the 5-day mean (i.e., pentad) dataset.

The remainder of the present study is organized as follows. The data and method utilized in this study are introduced briefly in Sect. 2. In Sect. 3, the general relationship between Korean summer precipitation and WNPAC is investigated. Then, the non-linear relationship between WNPAC and Korean summer precipitation is investigated based on four different categories and their distinct physical features are described in Sect. 4. The final section summarizes and discusses the findings of the present study.

2 Data and method

Daily precipitation records collected from 61 weather stations by Korea Meteorological Administration (KMA) for the period of 1979–2017 are mainly analyzed to identify Korean precipitation variability. To investigate subseasonal variation, the daily dataset are converted to 5-day mean pentad dataset. The large scale precipitation structures are investigated based on the Climate Prediction Center (CPC) Merged Analysis of Precipitation (CMAP; Xie and Arkin 1997) pentad data from 1979 to 2016. Pentad mean SST data are calculated from the National Oceanic and Atmospheric Administration (NOAA) daily Optimum Interpolation SST version 2 (OISST v2; Reynolds et al. 2002) which is available from September 1981. For calculation efficiency, the high resolution of $0.25° \times 0.25°$ is aggregated onto a $1° \times 1°$ grid. For additional analysis, the monthly mean SST data are obtained from NOAA Extended Reconstruction SST version 4 (Huang et al. 2015). Pentad means of geopotential height, wind vector, relative humidity and air temperature are also calculated by the daily analyses of the National Centers for Environmental Prediction/Department of Energy (NCEP/DOE) reanalysis 2 (Kanamitsu et al. 2002) for the period of 1979–2017. To estimate the moisture flux, the vertically integrated moisture flux ($\vec{Q}$) is calculated as $\vec{Q} = \frac{1}{g}\int_{p_t}^{p_s} q\vec{V}\, dp$, where q is specific humidity, $\vec{V}$ is horizontal wind vector, p_s is surface pressure, p_t is pressure at the top of the atmospheric layer and g is the gravitational acceleration. In this study, the vertical integration is performed from surface to 300 hPa.

The conditional composite analyses for the four categories based on the phase relationship between Korean summer precipitation and WNPAC are mainly performed. The four categories constitute positive Korean precipitation combined with positive (negative) WNPAC, and negative Korean precipitation combined with positive (negative) WNPAC. The statistical significances of the composite anomalies are determined by the Student's *t* test.

3 The relationship between WNPAC and Korean summer precipitation

To delineate the variability of WNPAC, the simple circulation indices based on low-level geopotential height anomaly averaged over maximum variability center of WNP have been widely used in the previous studies (e.g., Lu and Dong 2001; Sui et al. 2007; Park et al. 2010; Yeo et al. 2012; Wang et al. 2013). Following the previous studies, this study also defines WNPAC index as 850 hPa geopotential height anomaly averaged over 110°–140°E, 10°–30°N where is the center of maximum variability. To unravel the relationship between WNPAC and Korean summer precipitation, we first calculate the simple correlation coefficients between WNPAC index and Korean precipitation averaged over 61 stations from pentad 32 (P32; 5th–9th June) to P49 (29th August–2nd September) during the period of 1979–2017 (Fig. 1a). Figure 1a shows that the WNPAC index is not significantly correlated with Korean precipitation on subseasonal time scales; the correlation coefficients in most pentads do not exceed 95% significance level. We further examine the relationship between Korean precipitation and WNPAC on monthly and seasonal timescales and compare it with the relationship between EASM and WNPAC (Fig. 1a). The correlation coefficients for June, July and August are 0.12, 0.05, and 0.37, respectively and that for summer mean (June–July–August; JJA) value is 0.04, which indicates that the relationship between Korean precipitation and WNPAC is insignificant both on seasonal and subseasonal timescales. However, the EASM variability, which is measured by averaged precipitation anomalies over 105°–145°E and 30°–45°N following Lee et al. (2005), is significantly correlated with WNPAC (r = 0.51 for JJA). This result is consistent with the previous studies, which reported high correlation coefficient of 0.92 (Wang et al. 2013) and 0.70 (Lee et al. 2013) between EASM and WNPAC. Note that the correlation coefficients between EASM and Korean precipitation for June, July, and August are − 0.07, 0.11, and − 0.25, respectively indicating substantial regional differences among EASM subcomponents. This result implies that there exists more complicated linkage between WNPAC and Korean precipitation, which is distinctive from the well-known relationship between WNPAC and EASM.

In order to clarify the relationship between WNPAC and Korean summer precipitation, the scatter diagram between the two during each summer pentad (P32–P49) for 1979–2017 is presented in Fig. 1b. As expected from Fig. 1a, the scatter plot exhibits diffused feature indicating insignificant linear relationship between WNPAC and Korean precipitation. Although linear relationship is obscure, a further examination is needed to identify whether there exists physically meaningful non-linear relationship between WNPAC and Korean precipitation. In other words, it should be investigated whether there exist different processes between the case that positive (negative) Korean precipitation anomaly accompanies with positive WNPAC anomaly and that with negative WNPAC anomaly. Therefore, we classify four categories based on the phase relationship between Korean precipitation and WNPAC. The four categories constitute positive Korean precipitation anomaly combined with positive (negative) WNPAC anomaly, which is referred as PosKP + PosWNP (PosKP + NegWNP) for convenience,

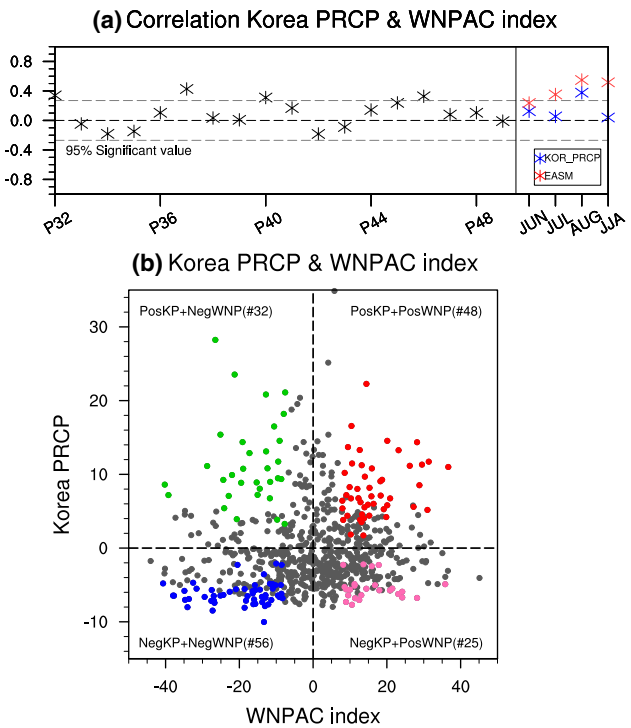

Fig. 1 **a** The correlation coefficients between precipitation anomalies averaged over 61 stations in Korea and WNPAC index from P32 to P49 during the period of 1979–2017 (black asterisks). The monthly mean values from June to August and seasonal mean (June–July–August) value are designated by blue asterisks while correlation coefficients between EASM and WNPAC indices are overlapped with red asterisks. **b** Scatter plot of Korean precipitation anomalies and WNPAC index from P32 to P49 during 1979–2017. The cases belong to four categories based on phase of Korean precipitation and WNPAC are designated by color dots as red, green, blue, and pink for PosKP + PosWNP, PosKP + NegWNP, NegKP + NegWNP, and NegKP + PosWNP, respectively

and negative Korean precipitation anomaly combined with positive (negative) WNPAC anomaly, which is referred to as NegKP + PosWNP (NegKP + NegWNP). For each pentad during summer (i.e., P32–P49), the positive (negative) Korean precipitation anomaly cases are selected in which Korean precipitation exceeds (falls) 80th (20th) percentile from 1979 to 2017. Meanwhile, a threshold of ±0.5 standard deviation of WNPAC index for each pentad during summer is applied for defining positive and negative WNPAC anomaly. By applying the above criteria, 48 (32) cases are detected as PosKP + PosWNP (PosKP + NegWNP) while 56 (25) cases are detected as NegKP + NegWNP (NegKP + PosWNP) and the corresponding cases are designated by red (green) and blue (pink) dots in Fig. 1b, respectively.

Figure 2 shows the occurrence frequency for the four categories by year and pentad. For the occurrence frequency by year, PosKP + PosWNP case frequently occurred from late-1980s to late-1990s showing maximum occurrence in 1998 (Fig. 2a). For the occurrence frequency by pentad, the notable feature is that NegKP + NegWNP case tends to occur more frequently in August (i.e., P45–P49) than in June and July (Fig. 2g), while NegKP + PosWNP case shows frequent occurrence in June and July than in August (Fig. 2h).

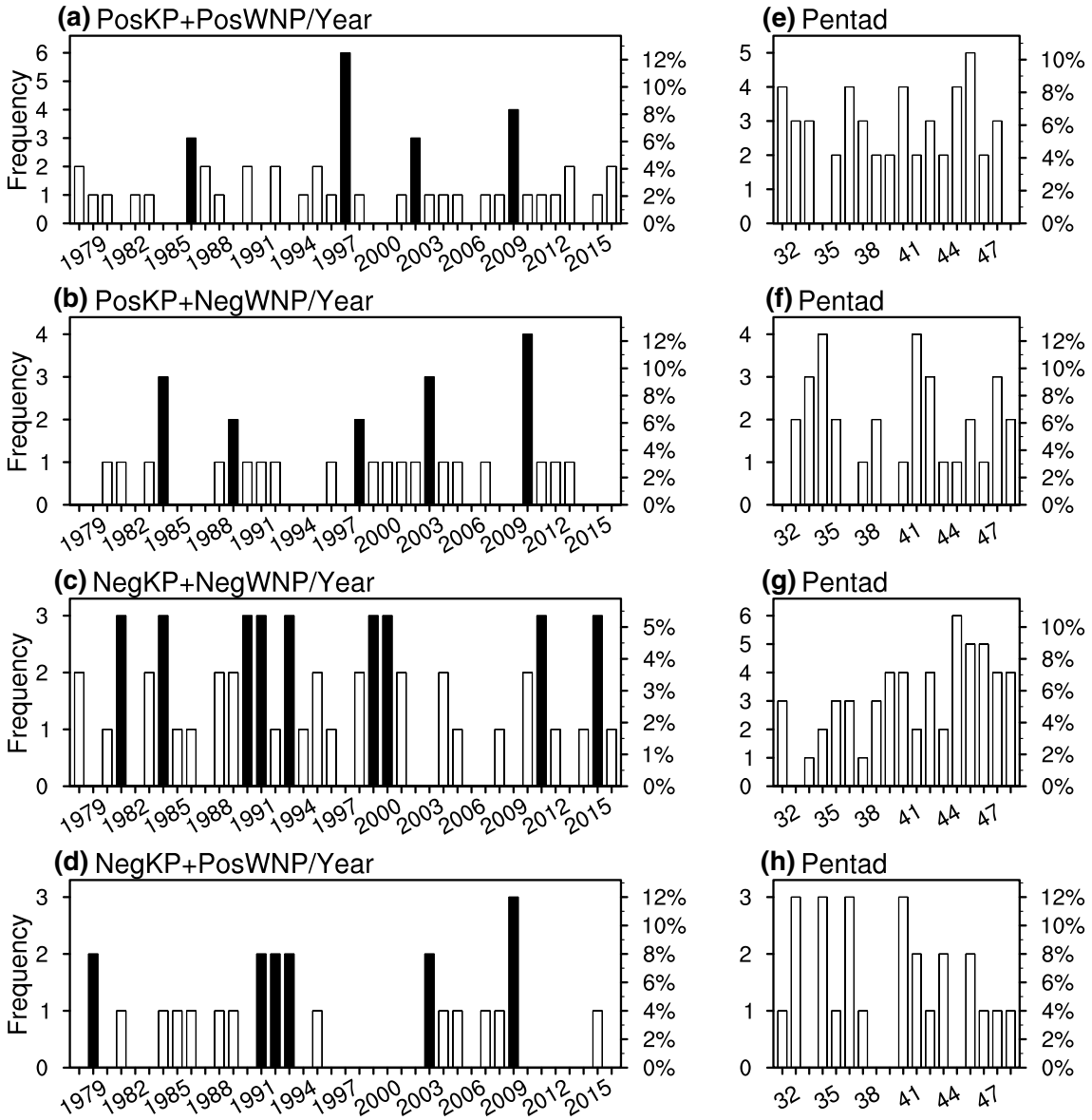

Fig. 2 The occurrence frequency of PosKP + PosWNP, PosKP + NegWNP, NegKP + NegWNP, and NegKP + PosWNP by year (**a**–**d**) and by pentad (**e**–**h**). The left axis indicates the number of occurrence while the right axis indicates occurrence ratio. The black bars in **a**–**d** are the years used for composite analyses in Figs. 4 and 9

4 Non-linear relationship between WNPAC and Korean summer precipitation

4.1 Positive Korean precipitation anomaly with different WNPAC phases

To investigate the non-linear relationship between WNPAC and Korean precipitation, we first focus on the cases of positive Korean precipitation with positive WNPAC anomaly and that with negative WNPAC anomaly (i.e., PosKP + PosWNP and PosKP + NegWNP). The composite patterns of 850 hPa geopotential height, precipitation, vertically integrated moisture transport and flux, SST and 850 hPa wind anomalies for PosKP + PosWNP and PosKP + NegWNP cases are presented in Fig. 3a–c and d–f, respectively. For PosKP + PosWNP case, significant positive geopotential height anomaly occupies not only over WNP region but also extends northeastward to North Pacific, showing broadly expanded enhanced subtropical high over North Pacific (Fig. 3a). The enhanced WNPAC is responsible for the suppressed precipitation and moisture divergence over its high pressure center. On the other hand, the excessive precipitation anomalies are elongated with banded structure along with the northwestern flank of WNPAC, corresponding to moisture convergence by anomalous southwesterly moisture transports (Fig. 3a, b). These moisture transports lead to more precipitation in the EASM region especially eastern China, Korea, and northern Japan. This result is consistent with the previous

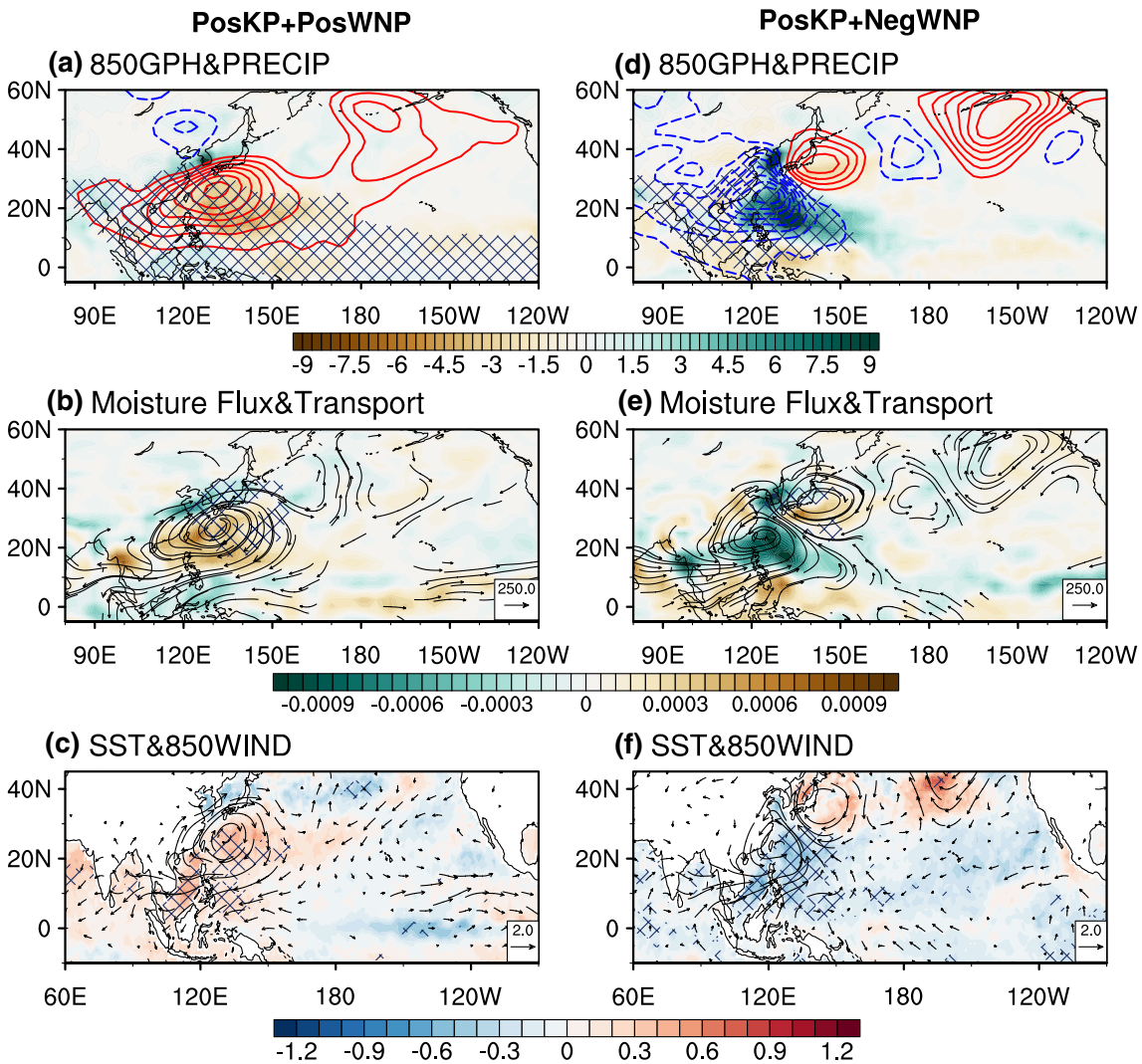

Fig. 3 Composite maps of **a**, **d** 850 hPa geopotential height (contour) and precipitation (shading) anomalies, **b**, **e** vertically integrated (from surface to 300 hPa) moisture transport (vector) and flux (shading) anomalies, **c**, **f** SST (shading) and 850 hPa wind (vector) anomalies for **a**–**c** PosKP + PosWNP and **d**–**f** PosKP + NegWNP, respectively. The statistically significant anomalies of 850 hPa geopotential height, moisture transport, and SST at 95% confidence level are indicated by diagonal lines

studies that the large amount of water vapor can be transported into East Asia along with the northwestern edge of WNPAC (Ninomiya and Kobayashi 1999; Lu and Dong 2001; Wang and Zhang 2002).

The SST anomaly pattern for PosKP + PosWNP exhibits warm SST anomalies over WNP region in conjunction with high pressure anomaly center (Fig. 3c). The suppressed convection associated with high pressure anomaly facilitates increased solar radiation via reduced cloud cover, which warms SST. On the other hand, cold SST anomalies are found over northern flank of WNPAC, which is associated with upward surface latent heat flux caused by positive precipitation anomalies. The prominent features of the composite SST field are the warm SST anomaly over northern Indian Ocean and cold SST anomaly over tropical central and eastern Pacific. This SST pattern resembles the general feature of decaying phase of El Niño. This result is consistent with the previous studies which reported that WNPAC frequently occurs during El Niño decaying summer (Wang et al. 2000; Chang et al. 2000) and accompanying Indian Ocean warming is instrumental in developing anomalous WNPAC (Li et al. 2008; Xie et al. 2009; Ding et al. 2010; Wu et al. 2010; Yun et al. 2013). It is suggested that atmospheric Kelvin waves induced by Indian Ocean warming drives Ekman divergence over WNP, which in turn produces suppressed convection and forms anomalous WNPAC (Xie et al. 2009; Wu et al. 2010). In addition to the Indian Ocean warming, the cooling of tropical central Pacific is also responsible for the enhancement of WNPAC through modulation of Walker circulation and local Hadley circulation (Wang et al. 2013).

To further confirm the SST evolution characteristics of PosKP + PosWNP case, the composite patterns of seasonal mean (three-month mean) SST anomalies for the years when occurrence of PosKP + PosWNP case exceeds 3 pentads, which corresponds to 6.5% of occurrence frequency, are investigated. The selected years are 1987, 1998, 2003, and 2010 (black bars in Fig. 2a) and the composite results from preceding winter (December–February; DJF) to the following summer (June–August; JJA) are presented in Fig. 4a–c. The strong El Niño pattern is prominent in preceding winter but this El Niño pattern quickly decays in spring and then mixed positive and negative SST anomalies take place over the tropical central and eastern Pacific in the following summer. Another notable feature is warm SST anomaly over Indian Ocean which lags the El Niño signal showing peak phase in summer. These seasonal evolution features of SST

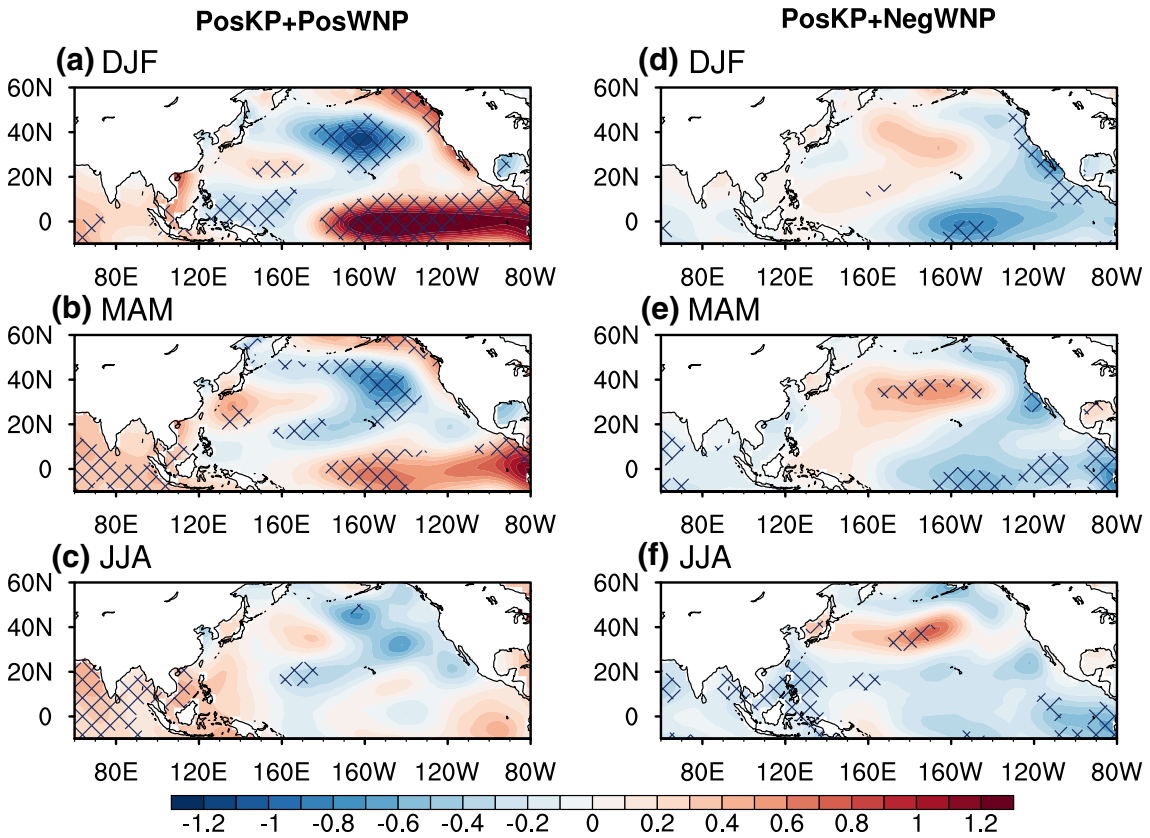

Fig. 4 Composite maps of seasonal (3-month) mean SST anomalies for **a–c** PosKP + PosWNP and for **d–f** PosKP + NegWNP from the preceding winter (DJF) to the following summer (JJA). The years that comprise composite is when the occurrence of PosKP + PosWNP (PosKP + NegWNP) is more than 3 (2) pentads. The statistically significant values at 90% confidence level are indicated by diagonal lines

for PosKP + PosWNP case further confirm that the development of WNPAC is closely related to the decaying phase of El Niño with significant warming in the Indian Ocean.

We next investigate the characteristic features for the case of positive Korean precipitation anomaly occurred with negative WNPAC anomaly (i.e., PosKP + NegWNP). The composite pattern of 850 hPa geopotential height anomaly presented in Fig. 3d shows that the negative WNPAC constitutes a part of wave train from WNP to west coast of North America, which resembles some part of PJ or East Asia–Pacific teleconnection pattern (e.g., Nitta 1987; Huang and Sun 1992; Kosaka and Nakamura 2006). This wave train pattern has been considered as northward propagation of Rossby waves driven by anomalous convective heating over the WNP (Nitta 1987; Huang and Sun 1992). Indeed, the well-organized enhanced precipitation and moisture convergence are evident over WNP region, which may trigger northward propagating Rossby waves. The wave propagation in turn forms the anomalous anticyclonic circulation to the east of Korea/Japan, which is responsible for positive precipitation anomaly in Korea through southeasterly moisture transport (Fig. 3d, e). The important role of anticyclonic circulation over east of Korea/Japan in transporting moisture into Korea has been also emphasized in the previous study of Lee and Seo (2013). Since the moisture is transported by southeasterly flow from WNP to Korea, precipitation over eastern China and Japan does not show positive anomalies. This is distinguishable result from the PosKP + PosWNP case, which shows zonally elongated rain band from eastern China to Japan (Fig. 3a, d).

The composite patterns of SST and 850 hPa wind anomalies for PosKP + NegWNP case are presented in Fig. 3f. As shown in this figure, cold (warm) SST anomalies are collocated with anomalous cyclonic (anticyclonic) circulation centers of the wave train. The positive precipitation anomalies over WNP cools SST through strengthening of surface evaporating cooling, while suppressed convection over high pressure center warms SST through increasing solar radiation via reduced cloud cover. This relationship indicates that SST variations are caused by overlying atmospheric variations. Meanwhile, SST over tropical Pacific exhibits neutral ENSO condition. To further investigate the seasonal evolution features of SST, the years when PosKP + NegWNP case occur more than 2 pentads, which corresponds to 6.5% of total occurrence, are selected (black bars in Fig. 2b). The selected years are 1985, 1990, 1999, 2004, and 2011, and their composite patterns are presented in Fig. 4d–f. The overall feature of SST evolution exhibits decaying phase of La Niña; La Niña-like SST anomalies are prominent during the preceding winter and spring but are weakened until summer. The SST evolution features of PosKP + NegWNP are distinctive from that of PosKP + PosWNP, showing La Niña decaying and El Niño decaying phase, respectively. Although the SST patterns for the two cases differ appreciably, they both show positive Korean summer precipitation anomalies, suggesting the non-linear relationship between Korean summer precipitation and ENSO, which is mediated by WNPAC.

One of important factors in controlling summer precipitation in Korea is the typhoon-induced precipitation event. Therefore, it is necessary to identify the contribution of typhoon-related precipitation event in two categories (i.e., PosKP + PosWNP and PosKP + NegWNP). It is speculated that the typhoon-related precipitation event contributes more to the PosKP + NegWNP than the PosKP + PosWNP since the enhanced convection over the WNP can provide a favorable condition for tropical cyclone genesis. Indeed, it is identified that 17 cases of the PosKP + NegWNP category are associated with the typhoon-related precipitation event, which corresponds to about 50% of total case. On the other hand, 6 cases are detected as typhoon-related precipitation in the PosKP + PosWNP, which is approximately 12% of total case, indicating substantial influence of typhoon-related precipitation on PosKP + NegWNP category. The detection of typhoon-related precipitation event in Korea is based on Typhoon White Book by KMA (2011), and the list of typhoon name of typhoon-related precipitation event for two categories is presented in Table 1.

Table 1 List of typhoon name for typhoon-related precipitation events in PosKP + PosWNP and PosKP + NegWNP categories

Category	Precipitation event (year, pentad)	Name of typhoon
PosKP + PosWNP	1979, P48	JUDY
	1987, P42	ALEX
	1991, P43	CAITLIN
	1993, P43	PERCY
	2010, P45	DIANMU
	2017, P37	NANMADOL
PosKP + NegWNP	1981, P49	AGNES
	1984, P49	JUNE
	1985, P45	KIT
	1985, P46	LEE
	1989, P42	JUDY
	1990, P35	OFELIA
	1990, P36	OFELIA
	1991, P47	GLADYS
	1993, P42	PERCY
	1999, P42	NEIL
	1999, P43	OLGA
	2002, P38	RAMMASUN
	2004, P46	MEGI
	2006, P39	EWINIAR
	2008, P41	ALMAEGI
	2011, P44	MUIFA
	2012, P48	BOLAVEN

4.2 Temporal evolution of positive Korean precipitation anomaly with different WNPAC phases

Besides the simultaneous circulation features of PosKP + PosWNP and PosKP + NegWNP cases, identification of their temporal evolution features is important for understanding development mechanism and improving prediction skill. To elucidate the temporal evolution features for PosKP + PosWNP case, composite anomalies of 850 hPa geopotential height and precipitation from 3-pentad before and 2-pentad after the peak phase are investigated in Fig. 5. At pentad − 3, enhanced and suppressed convections are found over west and east of Maritime continent, respectively. During this period, however, the atmospheric circulation pattern is not evident over WNP region (Fig. 5a). In the next pentad, the convection structure seen in the previous pentad is more strengthened and the suppressed convection moves slightly northward toward WNP. Accordingly, weak anomalous anticyclonic circulation appears over western Pacific between 10°N and 20°N (Fig. 5b). The suppressed convection is further intensified and thus well-organized WNPAC develops in pentad − 1. In the meantime, the enhanced convection over west of Maritime continent is markedly weakened (Fig. 5c). During its peak phase, the pronounced WNPAC and moisture transport into East Asia along the northwestern flank of WNPAC is evident and this structure is maintained to some extent by pentad + 1. During these periods, the convection around Maritime continent is vague (Fig. 5d, e). Although the high pressure anomaly over WNP sustains by pentad + 2, it moves northward to cover East Asia and the moisture cannot be transported into East Asia. Also the suppressed convection over WNP becomes significantly weak (Fig. 5f). As a whole, the WNPAC develops in accordance with the intensification and northward movement of suppressed convection over tropical western Pacific.

The temporal evolution features of PosKP + NegWNP case are shown in Fig. 6. From pentad − 3 to pentad − 2, the precipitation anomalies show the suppressed convection over eastern Indian Ocean and enhanced convection over tropical western Pacific. During this period, the low pressure anomalies are collocated with the enhanced convection

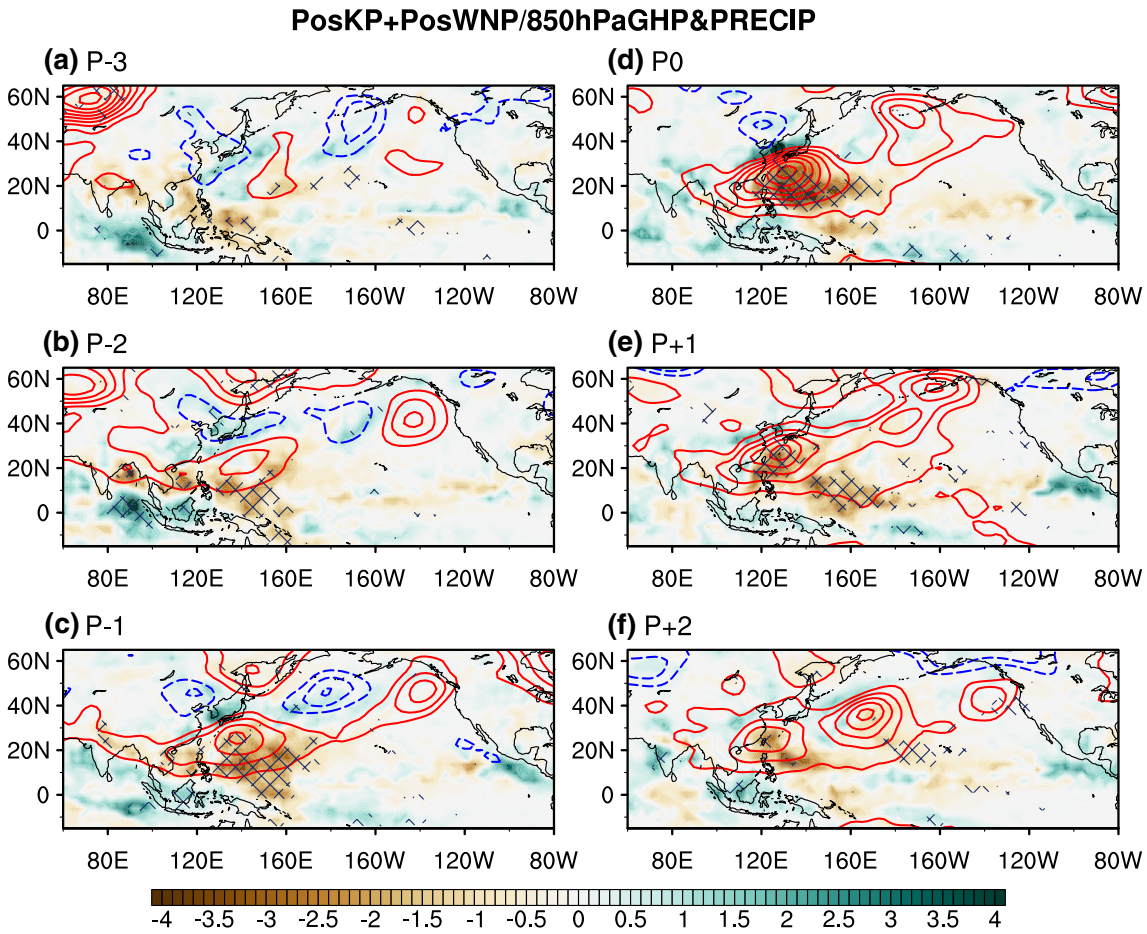

Fig. 5 Composite maps of 850 hPa geopotential height (contour) and precipitation (shading) anomalies from 3-pentad prior to 2-pentad after the peak phase of PosKP + PosWNP. The statistically significant anomalies of precipitation at 90% confidence level are indicated by diagonal lines

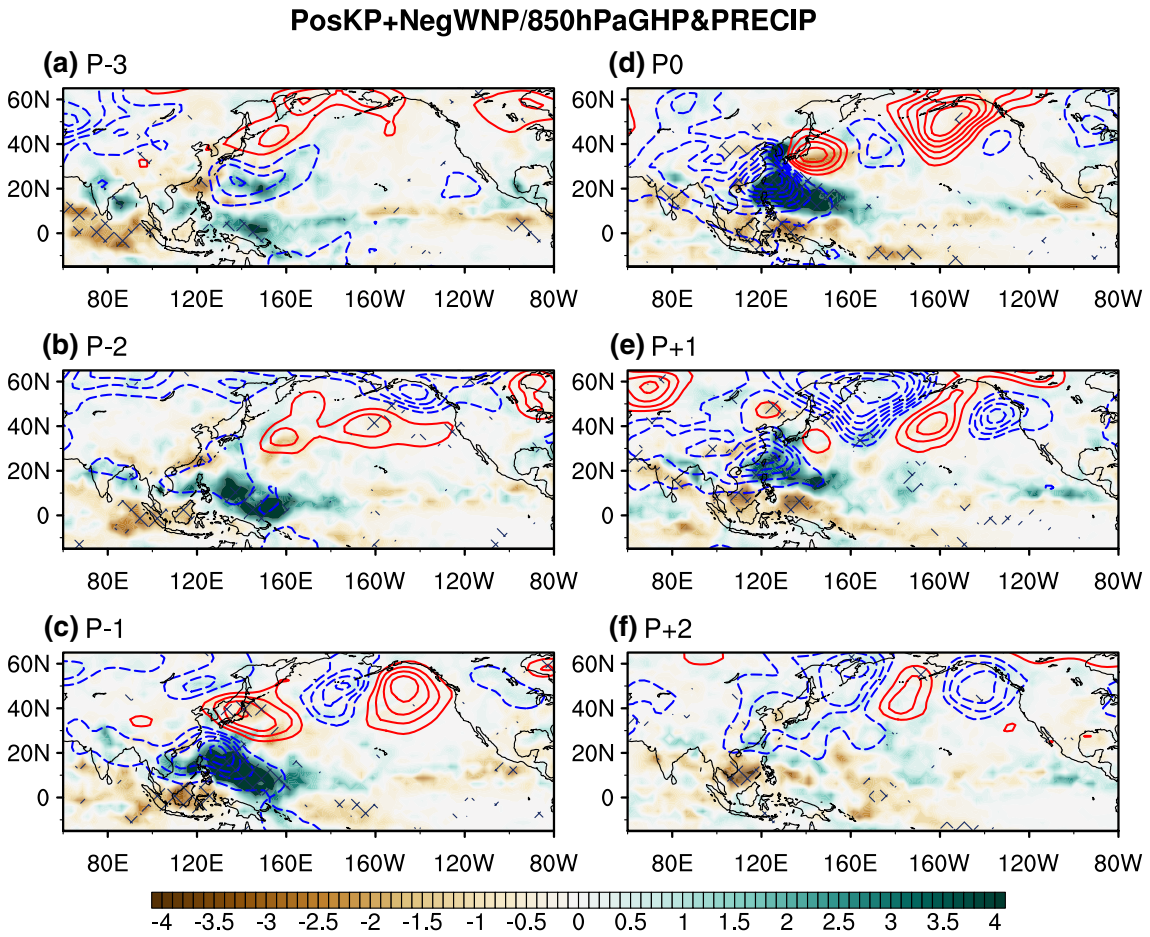

Fig. 6 Same figure as in Fig. 5 but for the PosKP + NegWNP case

centers but overall atmospheric circulation features do not exhibit distinct wave structure (Fig. 6a, b). On pentad − 1, the convection structure over Indo-western Pacific becomes more compact and slightly moves northeastward. At the same time, the prominent wave-like atmospheric structure from WNP to west coast of North America is developed. However, moistures are not sufficiently transported into Korea because Korea is mainly affected by high pressure anomaly (Fig. 6c). During its peak phase, the enhanced convection over WNP further moves northward while the suppressed convection over Maritime continent moves eastward showing meridional dipole convection structure. This structure is distinguishable from the zonal dipole convection structure seen in the pentad − 3 and pentad − 2. In this period, since Korea is located over the eastern (western) flank of low (high) pressure anomaly, sufficient moisture can be transported into Korea along with the southerly flow (Fig. 6d). However, the well-organized atmospheric wave structure is gradually collapsed from the pentad + 1 and this structure almost disappears in the pentad + 2. The enhanced convection over WNP is also weakened in the pentad + 1 and is obscure in the pentad + 2 (Fig. 6e, f).

Since the main focus of this study is Korean summer precipitation variability, we next investigate the differences in evolution feature of Korean precipitation between PosKP + PosWNP and PosKP + NegWNP. Figure 7 shows the pentad precipitation anomalies averaged over 61 stations in Korea during pentad − 3 to pentad + 3 relative to the pentads of PosKP + PosWNP and PosKP + NegWNP cases, which are designated as red and green bars, respectively. As shown in this figure, PosKP + NegWNP case exhibits larger amplitude of precipitation than the PosKP + PosWNP case during peak phase. However, significant positive precipitation anomalies are found from pentad − 2 to pentad + 1 for PosKP + PosWNP case, but there are no significant precipitation anomalies before peak phase for PosKP + NegWNP case. Instead, significant positive anomalies are maintained by pentad + 1 but it turns negative anomaly in pentad + 2 for PosKP + NegWNP case. Note, however, that the positive anomaly appears again in pentad + 3. In general, the temporal evolution features of Korean precipitation for PosKP + PosWNP case is characterized by moderate intensity of precipitation which lasts relatively long period while that for PosKP + NegWNP case displays strong intensity of

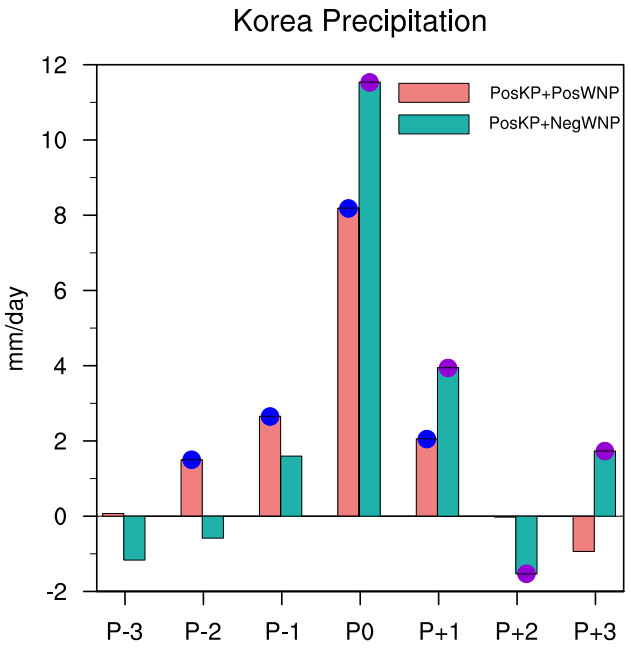

Fig. 7 Temporal evolution of Korean precipitation anomalies during 3-pentad before and 2-pentad after relative to the peak phase of PosKP + PosWNP (red bars) and that of PosKP + NegWNP (green bars). Blue and purple dots indicate statistically significant value at 80% confidence level

precipitation in relatively short period. It is also noteworthy that the evolution of Korean precipitation is dynamically consistent with the atmospheric circulations shown in Figs. 5 and 6.

4.3 Negative Korean precipitation anomaly with different WNPAC phases

We next investigate detailed features of the atmospheric and oceanic variations for the cases of negative Korean precipitation anomaly with different phases of WNPAC. Figure 8 is the same figure as in Fig. 3 except for the NegKP + NegWNP and NegKP + PosWNP cases. The atmospheric circulation pattern for NegKP + NegWNP case displays some similarities and differences not only with the PosKP + PosWNP case but also with the PosKP + NegWNP. The similar feature with PosKP + PosWNP except for the sign is that the low pressure anomaly in WNP (i.e., negative WNPAC anomaly) broadly extends from 90°E to 160°E with zonal direction which is accompanied with enhanced rainfall over WNP and suppressed rainfall over Korea. The negative precipitation anomaly over Korea is induced by moisture divergence in relation to the anomalous easterly moisture transport (Fig. 8b). However, atmospheric circulation for NegKP + NegWNP exhibits wave-like pattern across North Pacific, which is dissimilar feature to the PosKP + PosWNP (Figs. 3a, 8a) but is rather similar to PosKP + NegWNP (Figs. 3d, 8a). It should be also noted, however, that the wave structure of NegKP + NegWNP differs from that of PosKP + NegWNP showing smaller wave number than PosKP + NegWNP case (Figs. 3d, 8a).

The SST anomaly pattern for NegKP + NegWNP shows cold SST anomalies over WNP in association with low pressure anomaly and weak positive anomalies over tropical central Pacific and North Pacific between 30°N and 40°N. The seasonal evolution features of SST are shown in Fig. 9a–c. The years used for composite are 1982, 1985, 1991, 1992, 1994, 2000, 2001, 2012, and 2016 when occurrence of NegKP + NegWNP case exceeds 3 pentads (black bars in Fig. 2c). As shown in this figure, significant ENSO evolution feature is not found. It appears that the atmospheric structure of NegKP + NegWNP is associated with enhanced convection over WNP, which is not closely connected with ENSO. It is noteworthy that PosKP + NegWNP case also shows enhanced convection over WNP but is closely related to the decaying phase of La Niña (Figs. 3, 4). This difference may contribute to the different atmospheric circulations between the two cases although they share the similar feature of enhanced convection over WNP. In addition, the differences in the location of convection center and amplitude in WNP may induce the different atmospheric structure between the two cases. This argument can be further supported by the previous studies, which have suggested that the slight differences of the anomalous convection centers in WNP can cause significant differences in large scale circulation over WNP and East Asia (Lu 2004; Kim et al. 2009; Lu and Lin 2009).

The NegKP + PosWNP category has the smallest cases (#25) among the four categories of interest. The atmospheric and oceanic circulation patterns for NegKP + PosWNP exhibit distinctive features from the other three categories. The high pressure anomaly over WNP extends northward covering East Asia including Korea and low pressure anomaly prevails from Okhotsk Sea to the Aleutians (Fig. 8d). Since Korea is affected by high pressure anomaly, moistures cannot be transported into Korea (Fig. 8e). The significant non-linear structures of circulation anomalies between PosKP + NegWNP and NegKP + PosWNP are distinctive from the relationship between PosKP + PosWNP and NegKP + NegWNP, which roughly shows antisymmetric (linear) circulation anomalies. In order to reveal the detailed features of the linear and non-linear components for the case when WNPAC and Korean precipitation are out-of-phase, the circulation anomalies for PosKP + NegWNP minus and plus those for NegKP + PosWNP are illustrated in Fig. 10, respectively. The difference, which represents the linear component of the out-of-phase relationship, shows the northward extended negative WNPAC covering East Asia and positive precipitation anomalies prevailing from WNP to Korea (Fig. 10a, b). These features signify that the

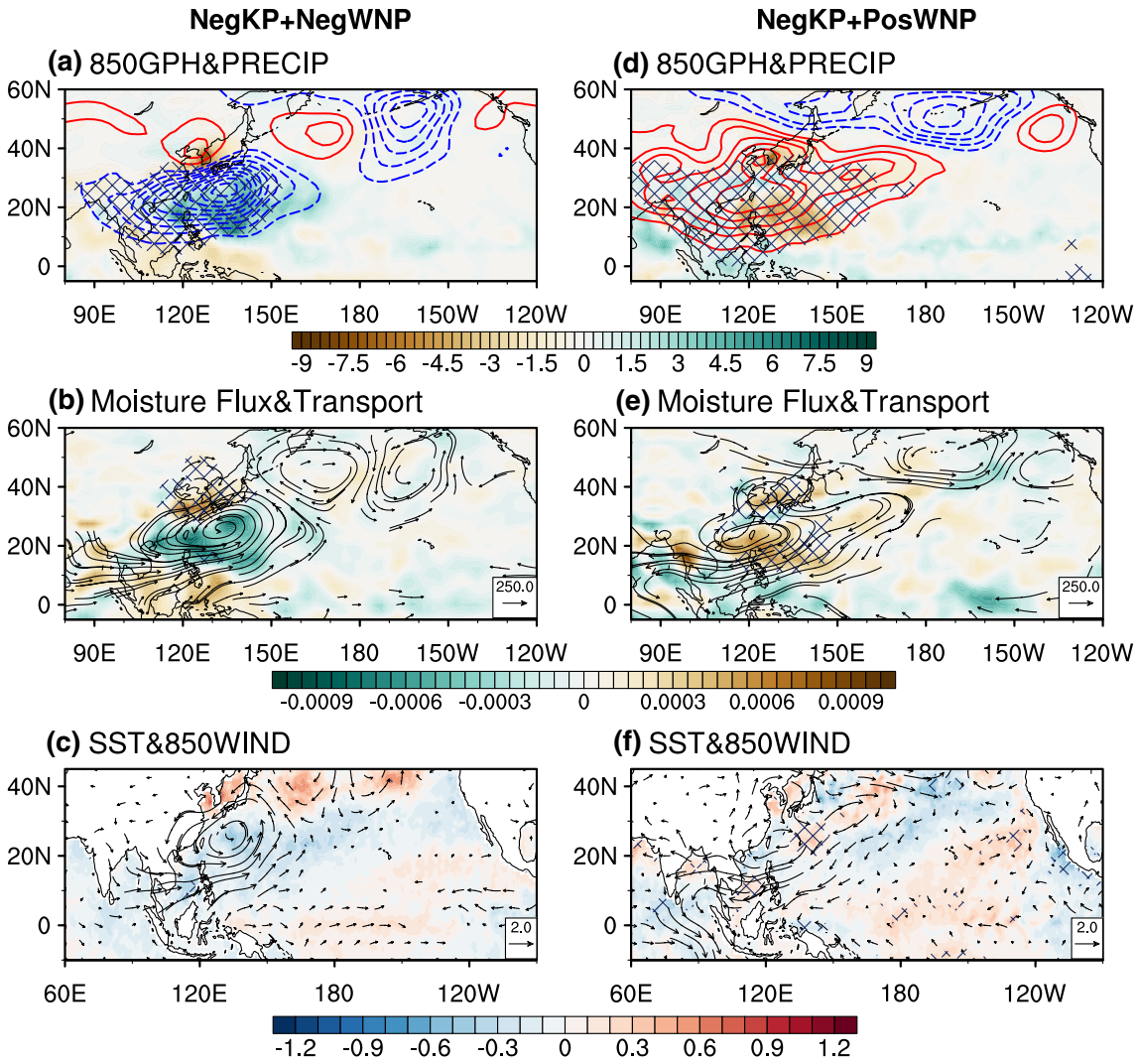

Fig. 8 Same figure as in Fig. 3 but for the NegKP + NegWNP and NegKP + PosWNP cases

linear part of the negative relationship between WNPAC and Korean precipitation can be explained such that northerly (southerly) flow along with the eastern flank of positive (negative) WNPAC leads to suppressed (enhanced) precipitation in Korea when WNPAC covers East Asia. On the other hand, the non-linear component between the PosKP + NegWNP and NegKP + PosWNP, which is shown as the sum of the two cases, exhibits wave-like structure along the North Pacific (Fig. 10c, d). This feature is similar to that of PosKP + NegWNP implying that enhanced Korean precipitation in relation to the wave-like atmospheric structure could be considered as non-linear component of the negative relationship between WNPAC and Korean precipitation. The substantial fraction of non-linear component is primarily attributed to the large influence of typhoon-related precipitation in PosKP + NegWNP case (Table 1).

The composite of SST for NegKP + PosWNP shows warm SST anomalies from northeastern Pacific to tropical central Pacific (Fig. 8f). The seasonal evolution features of SST are displayed in Fig. 9d–f. The years that comprise composite are 1980, 1992, 1993, 1994, 2004, and 2010, when the occurrence of NegKP + PosWNP are more than 2 pentads (black bars in Fig. 2d). The SST pattern during preceding winter presents significant warming over tropical central Pacific and cooling over tropical western to central North Pacific. However, there are no significant SST anomalies over Indian Ocean. Note that the SST pattern over tropical Pacific closely resembles the central Pacific (CP) El Niño, which shows largest SST anomalies over the tropical central Pacific. The CP El Niño pattern gradually decays in spring and this signal becomes vague in summer. The overall pattern of SST evolution for NegKP + PosWNP is characterized

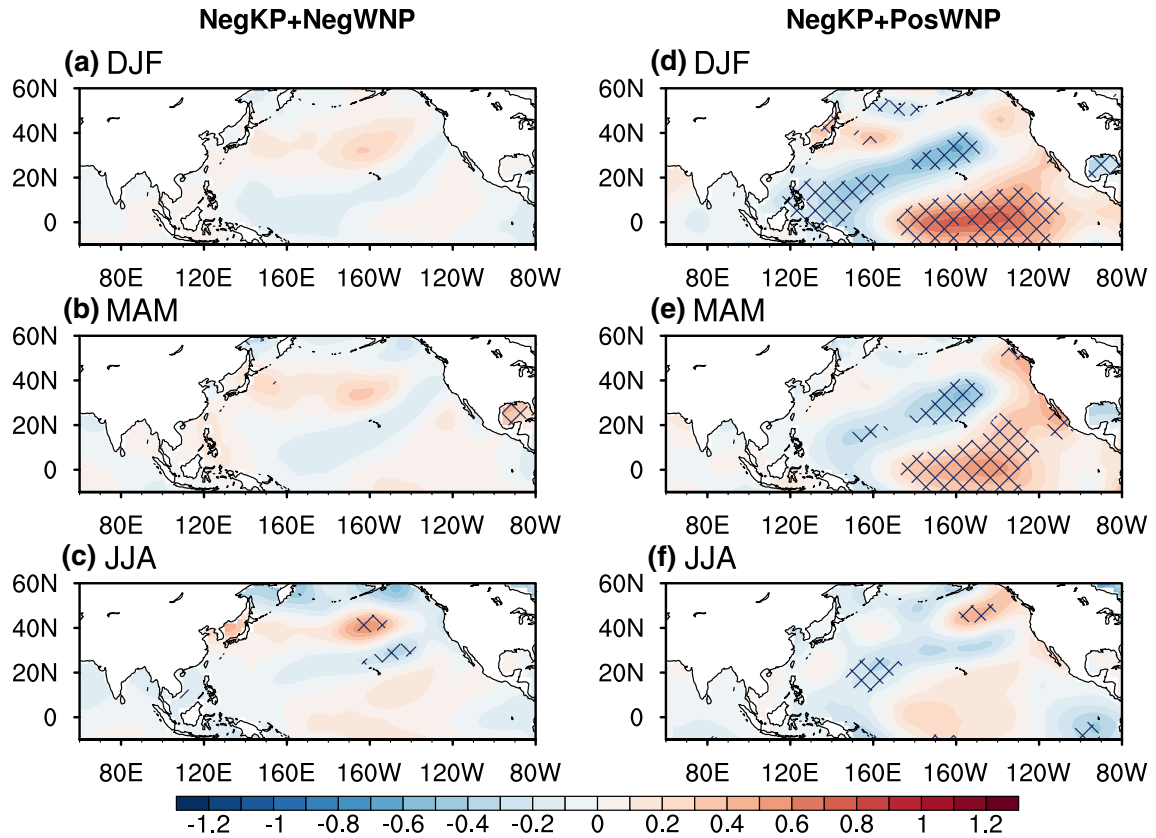

Fig. 9 Same figure as in Fig. 4 but for the NegKP + NegWNP and NegKP + PosWNP cases. The years that comprise composite is when the occurrence of NegKP + NegWNP (NegKP + PosWNP) is more than 3 (2) pentads

by decaying phase of CP El Niño (Fig. 9d–f). This is distinguishable feature from PosKP + PosWNP case which shows decaying phase of El Niño with maximum warming over tropical eastern Pacific accompanying with Indian Ocean warming (Fig. 4a–c). It is noteworthy that SST features over the North Pacific also differ significantly between PosKP + PosWNP and NegKP + PosWNP. The North Pacific SST for PosKP + PosWNP is characterized by zonal tripole pattern from western to eastern North Pacific during winter and summer (Fig. 4a, b), while that for NegKP + PosWNP shows negative SST anomaly, which is slightly tilted in the southwest direction (Fig. 9d, e). The different types of El Niño evolution and different influence of Indian Ocean may result in the differences in the convection amplitude and location over WNP, which drives different atmospheric response in the mid-latitude between PosKP + PosWNP and NegKP + PosWNP. In addition, the different features of SST over North Pacific may also affect different configurations of WNPAC for the two categories.

4.4 Temporal evolution of negative Korean precipitation anomaly case

In this subsection, the temporal evolution features of NegKP + NegWNP and NegKP + PosWNP are described in comparison with positive Korean precipitation anomaly cases. Figure 11 shows the temporal evolution of 850 hPa geopotential height and precipitation anomalies for NegKP + NegWNP case. At pentad − 2, positive precipitation anomaly is found over WNP and atmospheric wave structure appears from WNP to North America (Fig. 11b). In the next two pentads, this wave structure is strengthened in accordance with the enhancement of convection over WNP (Fig. 11c, d). The wave structure starts to collapse from pentad + 1 in conjunction with weakening of convection over WNP (Fig. 11e, f). The major difference in the evolution of NegKP + NegWNP from that of PosKP + NegWNP, which also shows the enhanced convection over WNP as a major component, is the standing feature of suppressed convection over Maritime continent in NegKP + NegWNP. Note that the suppressed convection in PosKP + NegWNP clearly shows the eastward movement from eastern Indian Ocean to Maritime continent (Fig. 6). This different evolution of

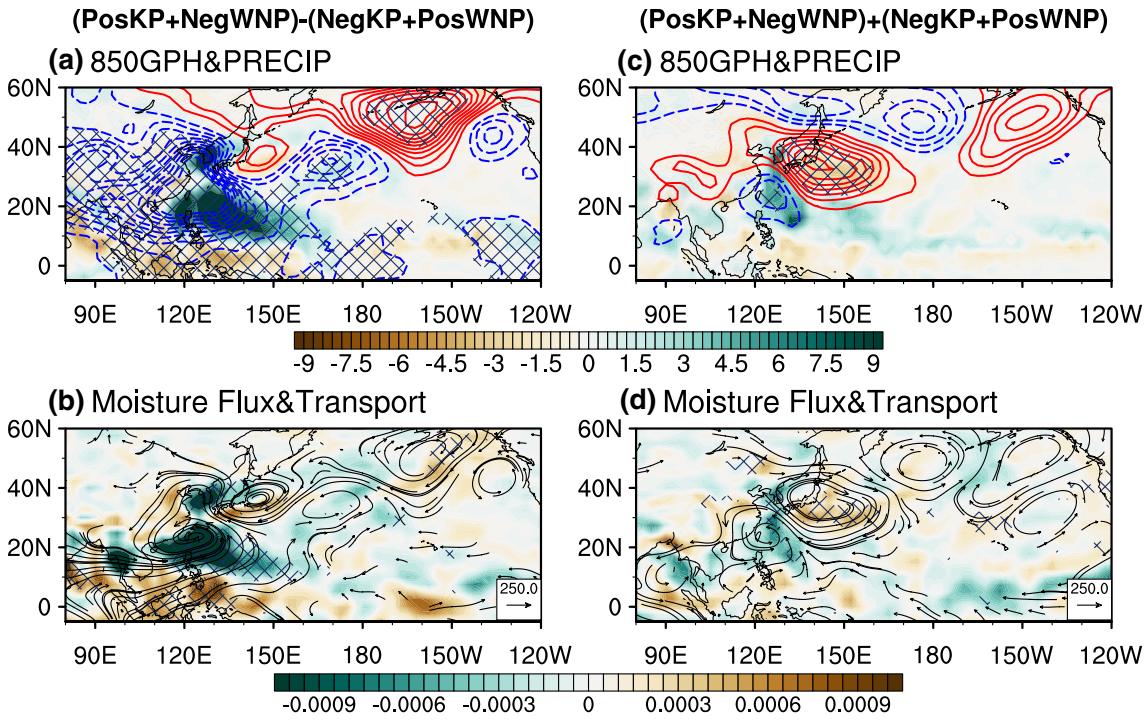

Fig. 10 Composite maps of **a**, **c** 850 hPa geopotential height (contour) and precipitation (shading) anomalies and **b**, **d** vertically integrated moisture transport (vector) and flux (shading) anomalies for **a**, **b** difference between PosKP + NegWNP and NegKP + PosWNP, which represent linear component, and **c**, **d** sum of PosKP + NegWNP and NegKP + PosWNP, which represent non-linear component. The statistically significant anomalies of 850 hPa geopotential height and moisture flux at 95% confidence level are indicated by diagonal lines

convection may affect different atmospheric wave structure, which results in different impact on Korean summer precipitation.

Meanwhile, the evolution of NegKP + PosWNP shows the zonal dipole pattern of convection between west and east of Maritime continent showing enhanced and suppressed convection, respectively at pentad − 2 (Fig. 12b). This convection structure is more amplified and suppressed convection moves northward toward WNP in the next pentads. Accordingly, the high pressure anomaly appears over WNP, which extends from Asian continent to eastern North Pacific (Fig. 12c). During its peak phase, the zonal dipole structure of convection moves further northward, and consequently high pressure anomaly covers East Asia, which results in negative precipitation anomaly over Korea (Fig. 12d). After its peak phase, the convection over WNP and the associated circulation are significantly weakened (Fig. 12e, f). The major difference of NegKP + PosWNP in comparison with PosKP + PosWNP is the significant enhanced convection over west of Maritime continent. Note that the enhanced convection over Maritime continent for PosKP + PosWNP becomes insignificant after pentad − 2 (Fig. 5). Although PosKP + PosWNP and NegKP + PosWNP share common feature of suppressed convection over WNP, the differences in the convective activity around Maritime continent between the two may act as probable source for different atmospheric response. However, additional analyses are needed for further clarification of the role of different western Pacific convection structure in affecting atmospheric response. We further investigate the evolution features of linear and non-linear components between PosKP + NegWNP and NegKP + PosWNP. The linear component estimated by the difference between the two, exhibits expansion of WNPAC into East Asia in accordance with the northward movement of convective activity over the WNP. On the other hand, the evolution features of non-linear component measured by the sum of two show development of wave structure in conjunction with enhanced convection in the WNP (figure not shown).

The evolution characteristics of Korean precipitation for NegKP + NegWNP and NegKP + PosWNP are presented in Fig. 13. As shown in this figure, NegKP + NegWNP case exhibits larger amplitude of negative precipitation anomaly than NegKP + PosWNP case. Also, NegKP + NegWNP displays more systematic evolution feature showing negative anomaly from pentad − 1 to pentad + 2, while NegKP + PosWNP shows significant negative anomaly only on its peak phase. The small case of NegKP + PosWNP as well as the evolution features shown in Fig. 13 suggests that the negative precipitation anomaly in Korea is more

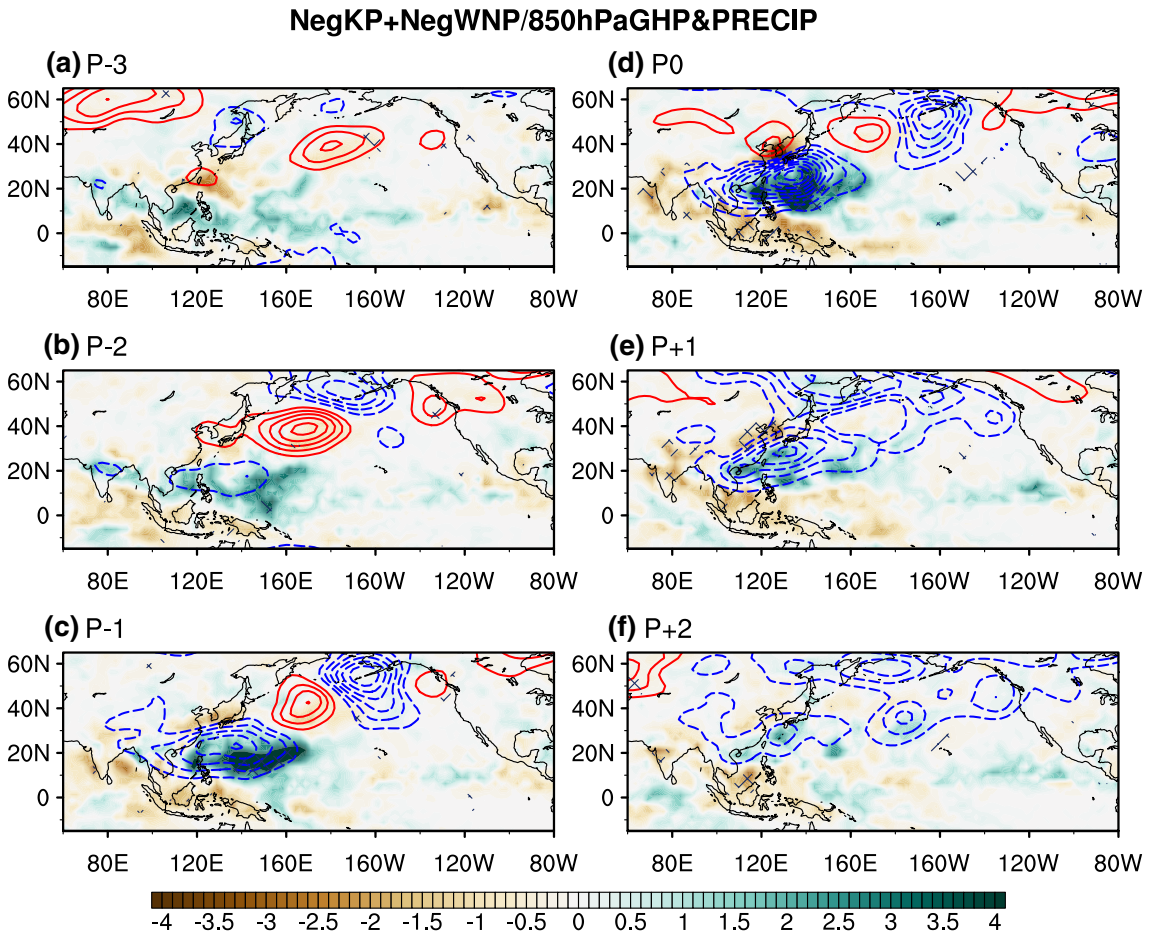

Fig. 11 Same figure as in Fig. 5 but for the NegKP + NegWNP case

dominantly influenced by negative WNPAC than positive WNPAC.

5 Summary and concluding remark

This study investigates the relationship between WNPAC and Korean summer precipitation on subseasonal time scale. Although there is no significant linear relation between WNPAC and Korean summer precipitation, the physically and dynamically meaningful atmospheric and oceanic circulation features are identified when we consider the non-linear relationship between the two. The positive and negative Korean summer precipitation anomaly cases are classified based on the different phases of WNPAC anomaly, which constitute PosKP + PosWNP, PosKP + NegWNP, NegKP + NegWNP, and NegKP + PosWNP. For the positive Korean precipitation anomaly accompanying with positive WNPAC anomaly (i.e., PosKP + PosWNP), the anomalous WNPAC is broadly expanded from WNP to North Pacific and moistures are transported into East Asia through southwesterly flow along the northwestern flank of WNPAC. In this case, the development of anomalous WNPAC is associated with the decaying phase of El Niño with Indian Ocean warming. Although the occurrence frequency is relatively low, there is a case that the development of WNPAC leads to suppressed Korean precipitation (i.e., NegKP + PosWNP) because Korea is affected by high pressure anomaly of northward expanded WNPAC. This type of WNPAC anomaly tends to develop under the conditions of decaying phases of CP El Niño without Indian Ocean influence. The differences in the convective activity over WNP in relation to different seasonal evolution of ENSO and different influence of Indian Ocean may lead to different structures of WNPAC, which results in different summer climate over Korea.

Meanwhile, the negative WNPAC anomaly, which is accompanied with enhanced convection over WNP, tends to constitute a wave-like atmospheric structure across the Pacific. This is distinguishable feature from positive WNPAC anomaly accompanying with suppressed

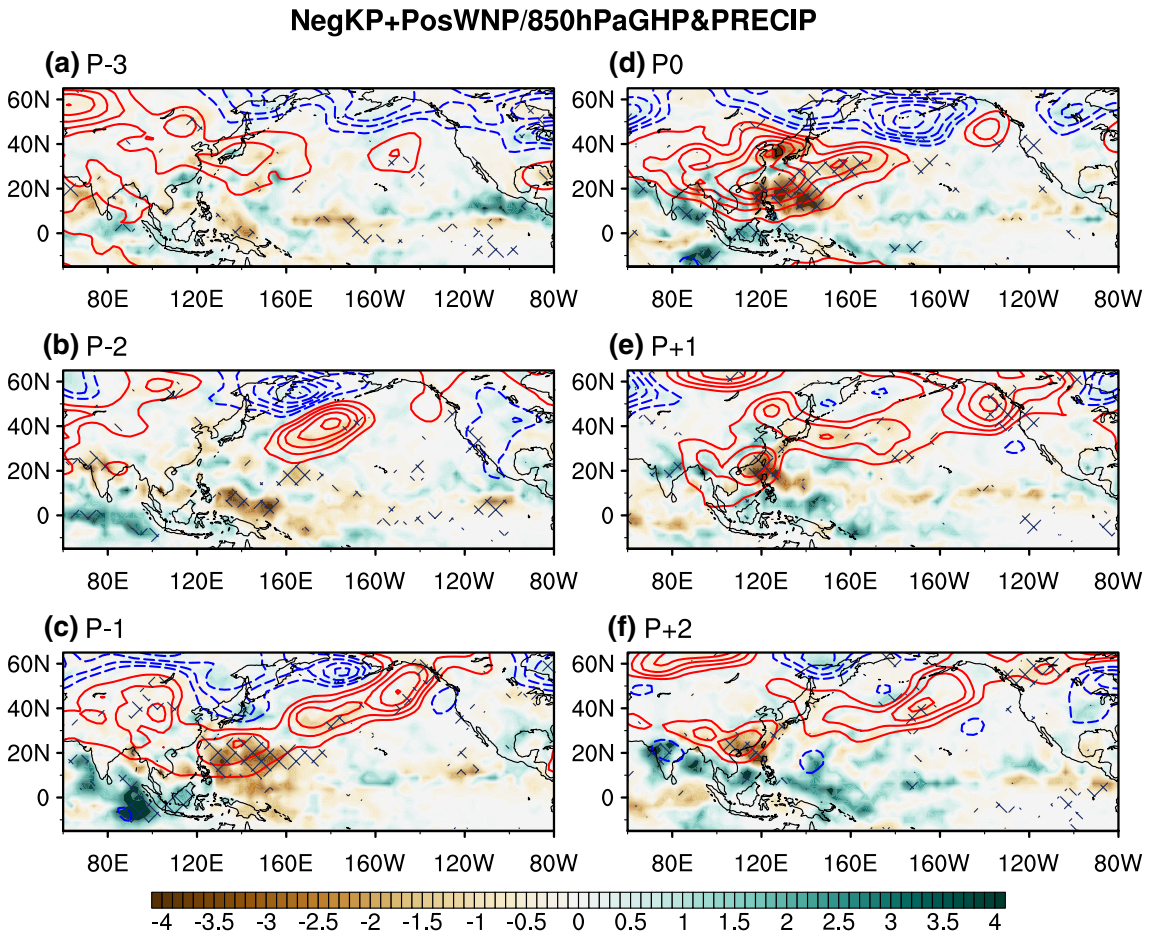

Fig. 12 Same figure as in Fig. 5 but for the NegKP + PosWNP case

convection over WNP, which does not show atmospheric wave structure. This result implies the asymmetry of atmospheric response between the enhanced and suppressed convection over WNP. The negative WNPAC anomaly can further be classified based on the different impact on Korean summer precipitation. When the negative WNPAC anomaly constitutes wave train with an anticyclonic circulation to the east of Korea, the moistures are transported into Korea through southeasterly flows along with the eastern (western) flank of low (high) pressure anomalies around Korea. In this case (i.e., PosKP + NegWNP), the seasonal evolution of SST is characterized by decaying phase of La Niña. It is also found that the typhoon-related precipitation substantially contributes to the Korean precipitation in this category. For the negative Korean precipitation anomaly accompanying with negative WNPAC anomaly (i.e., NegKP + NegWNP), easterly flow along with the northern flank of negative WNPAC leads to suppressed precipitation in Korea. The development of this type of negative WNPAC is not closely related to the distinct ENSO evolution features.

In summary, four categories based on the relationship between WNPAC and Korean summer precipitation exhibit distinctive atmospheric and oceanic circulation features. In particular, the discernable seasonal evolution patterns of SST in relation to ENSO for four categories provide the basis for the seasonal prediction on Korean summer precipitation. This non-linear relationship between WNPAC and Korean precipitation cannot be identified from the linear techniques such as regression or empirical orthogonal function analyses.

Since the present analyses are mainly based on the WNPAC index, which is defined by regionally averaged 850 hPa geopotential height anomalies, the concerning issue is how the results are sensitive to the different regions for defining WNPAC index. For this issue, we conducted the analyses with slightly different WNPAC index (i.e., 100°–150°E, 10°–30°N) and the results are not overly sensitive to the slight difference of WNPAC index (figure not shown). Note, however, that the WNPAC index used in this study has advantages in capturing and distinguishing major features of different structures of WNPAC. We also

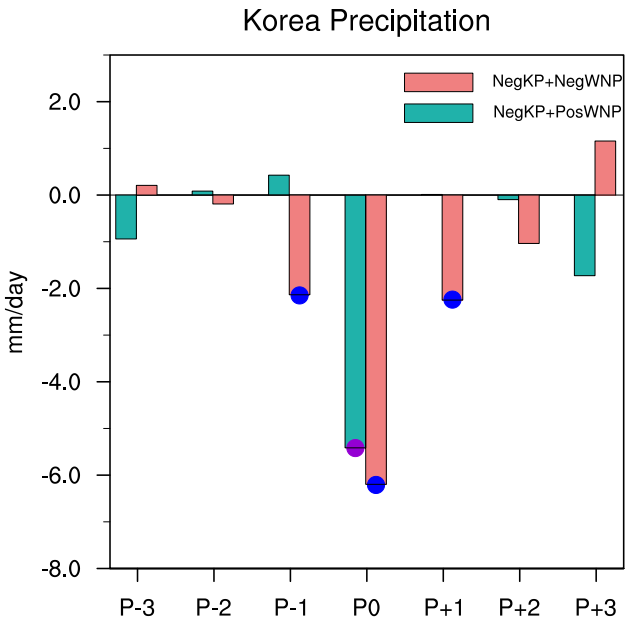

Fig. 13 Same figure as in Fig. 7 but for the NegKP + NegWNP and NegKP + PosWNP case

tested the sensitivity of results to the timescale of dataset. This study used 5-day mean pentad dataset to understand subseasonal variability of Korean precipitation in relation to WNPAC. Thus, the results may contain influence of the synoptic scale disturbances. In order to clarify whether the results are sensitive to the influence of synoptic disturbances, the present results are re-examined by using 10-day averaged dataset. The results are virtually identical with those in Sect. 4, indicating that the present results are statistically significant variability on subseasonal time scale (figure not shown).

The results of the present study are mainly obtained from composite analysis. In order to provide robustness of the results, further evaluations on the dynamical process of different relationship between WNPAC and Korean summer precipitation are still needed. For instance, the idealized model experiment with different SST forcing in relation to ENSO is needed to identify how the SST contributes differently to the structure of WNPAC that have different impact on Korean precipitation. Furthermore, this study mainly focuses on the western North Pacific variability (i.e., WNPAC) for understanding Korean precipitation. However, since Korean precipitation is largely affected by other factors such as mid-latitude wave train (Lee and Ha 2015; Park et al. 2015) additional analyses on the various factors affecting Korean precipitation should be conducted for more comprehensive understanding on Korean summer precipitation variability.

Acknowledgements This work is supported by APEC Climate Center.

References

Chang CP, Zhang Y, Li T (2000) Interannual and interdecadal variations of the East Asian summer monsoon and tropical Pacific SSTs. Part I: roles of the subtropical ridge. J Clim 13(24):4310–4325

Chowdary JS, Xie SP, Luo JJ, Hafner J, Behera S, Masumoto Y, Yamagata T (2011) Predictability of northwest Pacific climate during summer and the role of the tropical Indian Ocean. Clim Dyn 36(3–4):607–621

Ding R, Ha KJ, Li J (2010) Interdecadal shift in the relationship between the East Asian summer monsoon and the tropical Indian Ocean. Clim Dyn 34(7–8):1059–1071

Guan Z, Yamagata T (2003) The unusual summer of 1994 in East Asia: IOD teleconnections. Geophys Res Lett 30(10):1544

Huang R, Sun F (1992) Impacts of the tropical western Pacific on the East Asia summer monsoon. J Meteorol Soc Jpn Ser II 70(1B):243–256

Huang R, Wu Y (1989) The influence of ENSO on the summer climate change in China and its mechanism. Adv Atmos Sci 6(1):21–32

Huang B et al (2015) Extended reconstructed sea surface temperature version4 (ERSSTv.4). Part I: upgrades and intercomparisons. J Clim 28(3):911–930

Kanamitsu M, Ebisuzaki W, Woollen J, Yang SK, Hnilo J, Fiorino M, Potter GL (2002) Ncep-doe amip-2 reanalysis (r-2). Bull Am Meteorol Soc 83(11):631–1643

Kang IS, Ho CH, Lim YK, Lau KM (1999) Principal modes of climatological seasonal and intraseasonal variations of the Asian summer monsoon. Mon Weather Rev 127:322–340

Kim JE, Yeh SW, Hong SY (2009) Two types of strong northeast Asian summer monsoon. J Clim 22(16):4406–4417

Kim W, Jhun JG, Ha KJ, Kimoto M (2011) Decadal changes in climatological intraseasonal fluctuation of subseasonal evolution of summer precipitation over the Korean peninsula in the mid-1990s. Adv Atmos Sci 28(3):591–600

Korea Meteorological Administration (KMA) (2011), Typhoon White Book. p. 358, 11-1360016-000001-01 **(in Korean)**

Kosaka Y, Nakamura H (2006) Structure of the dynamics of the summertime Pacific-Japan teleconnection pattern. Q J R Meteorol Soc 132(619):2009–2030

Lau NC, Nath MJ (2003) Atmosphere-ocean variations in the Indo-Pacific sector during ENSO episodes. J Clim 16(1):3–20

Lee JY, Ha KJ (2015) Understanding of interdecadal changes in variability and predictability of the Northern Hemisphere summer tropical-extratropical teleconnection. J Clim 28:8634–8647

Lee SE, Seo KH (2013) The development of a statistical forecast model for Changma. Weather Forecast 28(6):1304–1321

Lee EJ, Jhun JG, Park CK (2005) Remote connection of the northeast Asian summer rainfall variation revealed by a newly defined monsoon index. J Clim 18(21):4381–4393

Lee EJ, Yeh SW, Jhun JG, Moon BK (2006) Seasonal change in anomalous WNPAC associated with the strong East Asian summer monsoon. Geophys Res Lett 33(21):L21702. https://doi.org/10.1029/2006GL027474

Lee SS, Seo YW, Ha KJ, Jhun JG (2013) Impact of the western North Pacific subtropical high on the East Asian monsoon precipitation and the Indian Ocean precipitation in the boreal summer. Asia-Pac J Atmos Sci 49(2):171–182

Lee JY, Kwon M, Yun KS, Min SK, Park IH, Ham YG, Jin EK, Kim JH, Seo KH, Kim W, Yim SY, Yoon JH (2017) The long-term variability of Changma in the East Asian summer monsoon system: a review and revisit. Asia-Pac J Atmos Sci 53(2):257–272

Li S, Lu J, Huang G, Hu K (2008) Tropical Indian Ocean basin warming and East Asian summer monsoon: a multiple AGCM study. J Clim 21(22):6080–6088

Lu R (2001) Interannual variability of the summertime North Pacific subtropical high and its relation to atmospheric convection over the warm pool. J Meteorol Soc Jpn Ser II 79(3):771–783

Lu R (2004) Associations among the components of the East Asian summer monsoon system in the meridional direction. J Meteorol Soc Jpn Ser II 82(1):155–165

Lu R, Dong B (2001) Westward extension of North Pacific subtropical high in summer. J Meteorol Soc Jpn Ser II 79(6):1229–1241

Lu R, Lin Z (2009) Role of subtropical precipitation anomalies in maintaining the summertime meridional teleconnection over the western North Pacific and East Asia. J Clim 22(8):2058–2072

Nigam S (1994) On the dynamical basis for the Asian summer monsoon rainfall-El Niño relationship. J Clim 7(11):1750–1771

Ninomiya K, Kobayashi C (1999) Precipitation and moisture balance of the Asian summer monsoon in 1991. J Meteorol Soc Jpn Ser II 77(1):77–99

Nitta T (1987) Convective activities in the tropical western Pacific and their impact on the Northern Hemisphere summer circulation. J Meteorol Soc Jpn Ser II 65(3):373–390

Park JY, Jhun JG, Yim SY, Kim W (2010) Decadal changes in two types of the western North Pacific subtropical high in boreal summer associated with Asian summer monsoon/El Niño-Southern Oscillation connections. J Geophys Res. https://doi.org/10.1029/2009JD013642

Park HL, Seo KH, Son JH (2015) Development of a dynamics-based statistical prediction model for the Changma onset. J Clim 28(17):6647–6666. https://doi.org/10.1175/JCLI-D-14-00502.1

Reynolds RW, Rayner NA, Smith TM, Stokes DC, Wang W (2002) An improved in situ and satellite SST analysis for climate. J Clim 15(13):1609–1625

Sui CH, Chung PH, Li T (2007) Interannual and interdecadal variability of the summertime western North Pacific subtropical high. Geophys Res Lett. https://doi.org/10.1029/2006GL029204

Wang B, Zhang Q (2002) Pacific-East Asian teleconnection. Part II: how the Philippine Sea anomalous anticyclone is established during El Niño development. J Clim 15(22):3252–3265

Wang B, Wu R, Fu X (2000) Pacific-East Asian teleconnection: how does ENSO affect East Asian climate? J Clim 13(9):1517–1536

Wang B, Xiang B, Lee JY (2013) Subtropical high predictability establishes a promising way for monsoon and tropical storm predictions. Proc Natl Acad Sci 110(8):2718–2722

Wang B, Lee JY, Xiang B (2015) Asian summer monsoon rainfall predictability: a predictable mode analysis. Clim Dyn 44(1–2):61–74

Wu R, Hu ZZ, Kirtman BP (2003) Evolution of ENSO-related rainfall anomalies in East Asia. J Clim 16(22):3742–3758

Wu B, Li T, Zhou T (2010) Relative contributions of the Indian Ocean and local SST anomalies to the maintenance of the western North Pacific anomalous anticyclone during the El Niño decaying summer. J Clim 23(11):2974–2986

Xie P, Arkin PA (1997) Global precipitation: a 17-year monthly analysis based on gauge observations, satellite estimates and numerical model outputs. Bull Am Meteorol Soc 78(11):2539–2558

Xie SP, Hu K, Hafner J, Tokinaga H, Du Y, Huang G, Sampe T (2009) Indian Ocean capacitor effect on Indo-western Pacific climate during the summer following El Niño. J Clim 22(3):730–747

Yang J, Liu Q, Xie SP, Liu Z, Wu L (2007) Impact of the Indian Ocean SST basin mode on the Asian summer monsoon. Geophys Res Lett 34(2):L02708

Yeo SR, Jhun JG, Kim W (2012) Intraseasonal variability of western North Pacific subtropical high based on the El Niño influence and its relationship with East Asian summer monsoon. Asia-Pac J Atmos Sci 48(1):43–53

Yun KS, Yeh SW, Ha KJ (2013) Distinct impact of tropical SSTs on summer North Pacific high and western North Pacific subtropical high. J Geophys Res 118(10):4107–4116

Zhang R, Sumi A, Kimoto M (1996) Impact of El Niño on the East Asian monsoon. J Meteorol Soc Jpn Ser II 74(1):49–62